Supplemental information for:

Membrane binding induces distinct structural signatures in the mouse complexin-1 C-terminal domain

Emily M. Grasso[a], Mayu Terakawa[a], Alex L. Lai[b], Ying Xue Xie[a], Trudy F. Ramlall[a], Jack H. Freed [b], David Eliezer[a]

[a]Department of Biochemistry, Weill Cornell Medicine, New York, NY, United States,

[b]Department of Chemistry and Chemical Biology, Cornell University, Ithaca, NY United States

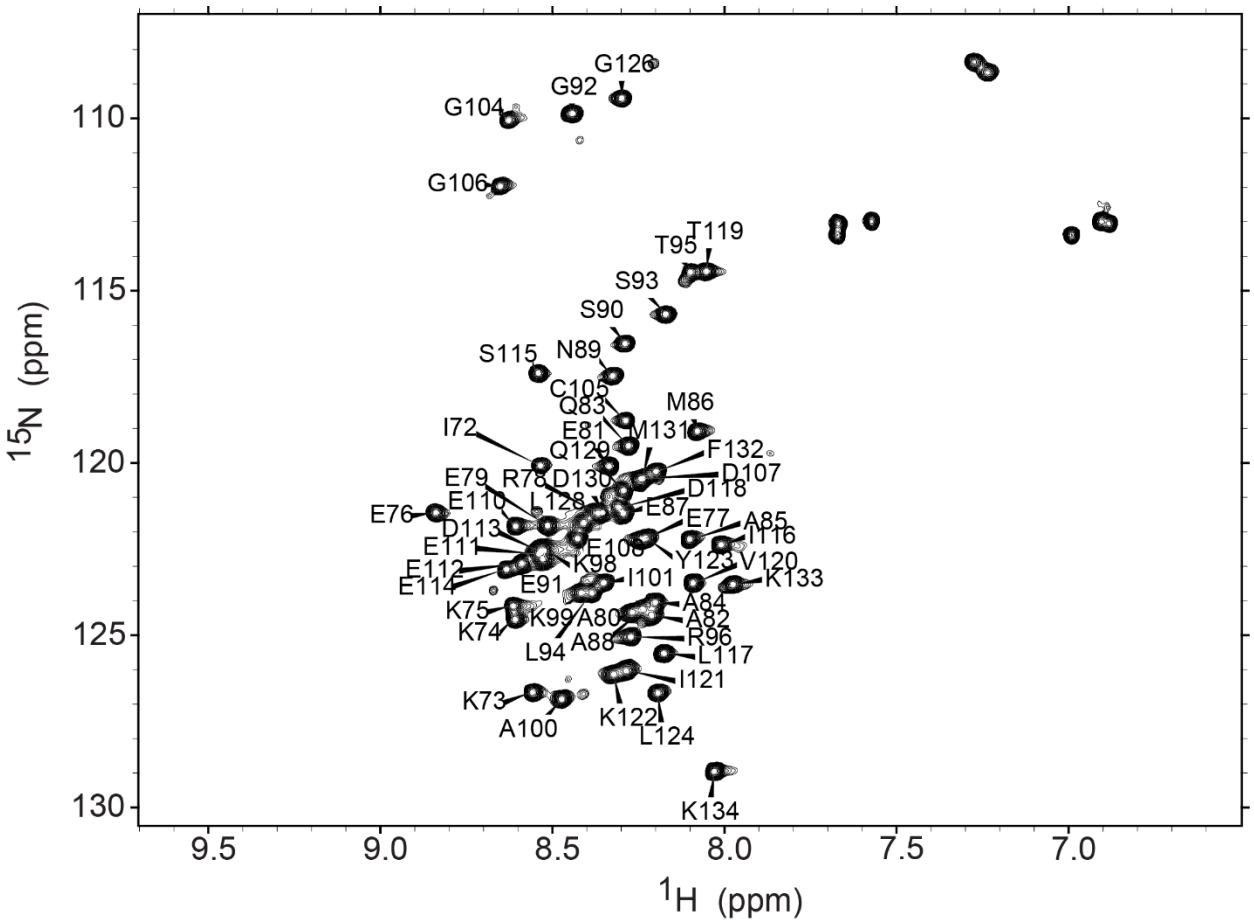

Figure S1 Assignments of free mCpx1 CTD Assigned 2D {^{15}N-^{1}H} HSQC spectrum of the mCpx1 CTD in the absence of any micelles. Spectrum was collected at 600 MHz (^{1}H) at 10°C with 32 scans and 174x2048 complex points.

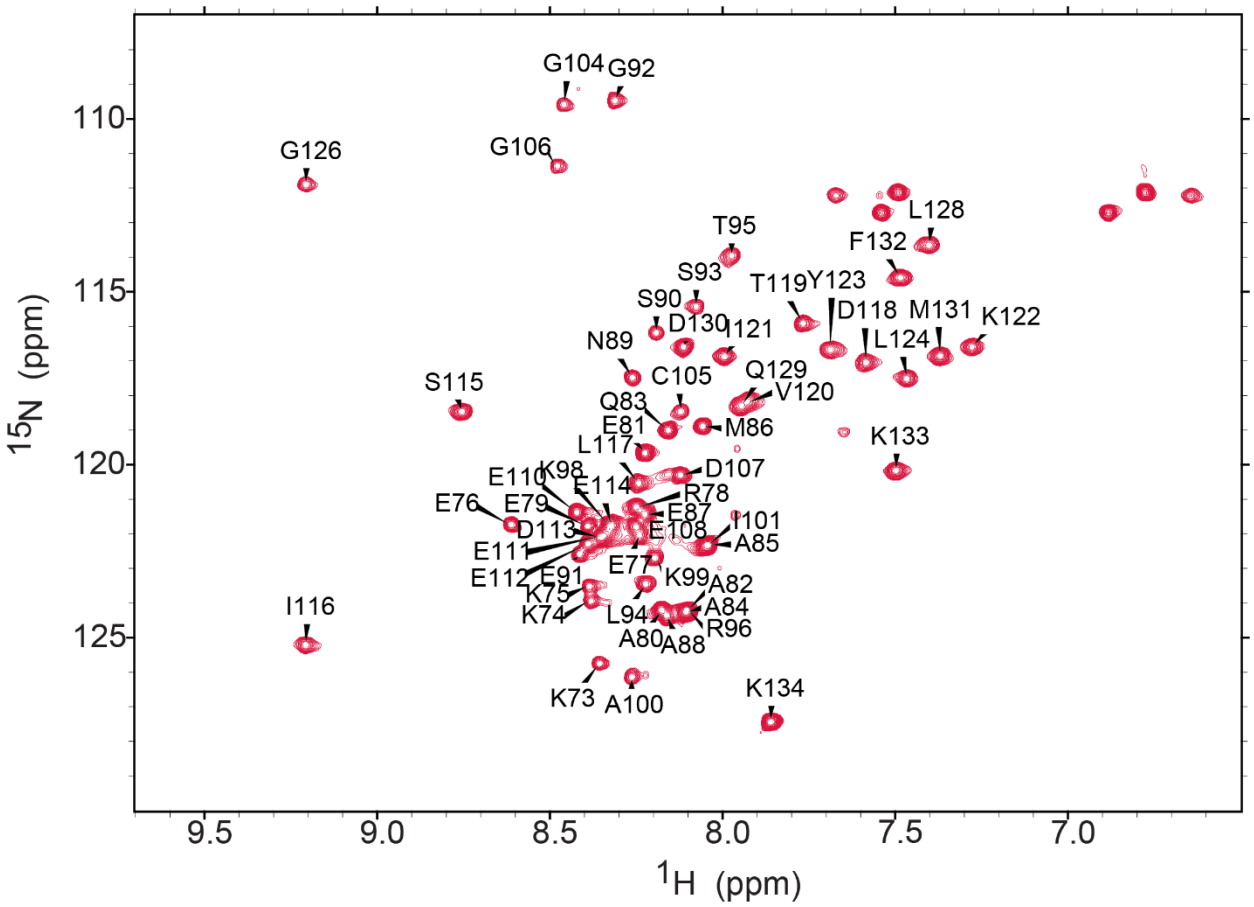

Figure S2 Assignments of the mCpx1 CTD in the presence of DPC micelles
Assigned 2D {^{15}N-^{1}H} HSQC spectrum of the mCpx1 CTD in the presence of DPC micelles. Spectrum was collected at 600 MHz (^{1}H) at 40°C with 32 scans and 174x2048 complex points.

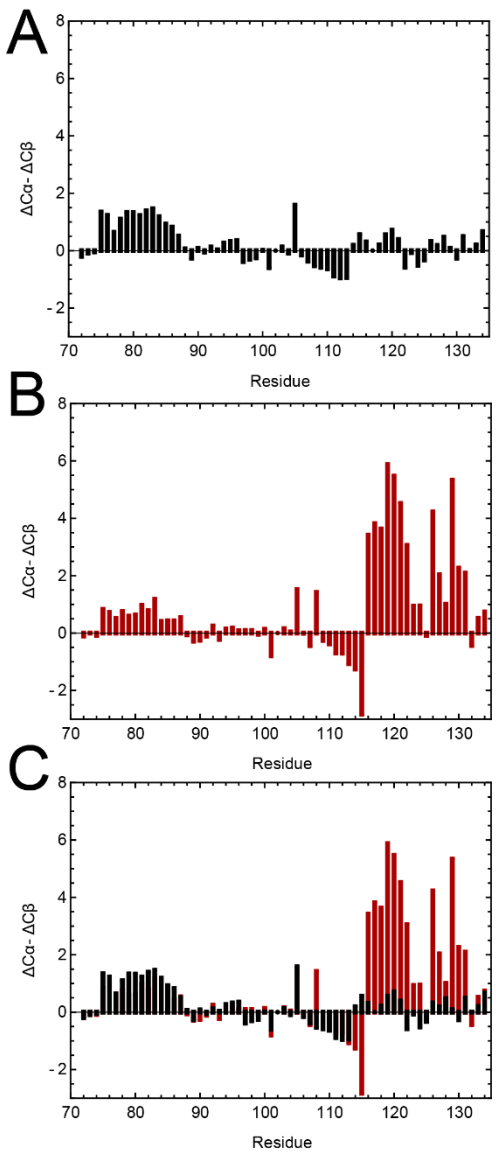

Figure S3 (A) ΔCα-ΔCβ plots for the free mCpx1 CTD indicate that the CTD is largely disordered, outside of residues ~75-85. (B) ΔCα-ΔCβ plots for micelle-bound mCpx1 CTD indicate that the mCpx1 CTD has a strong propensity for helical structure in its terminal ~20 residues in the presence of micelles. (C) Overlay of (A) and (B) emphasizes that the propensity helical structure in the terminal ~20 residues of the CTD only occurs in the presence of lipid micelles.

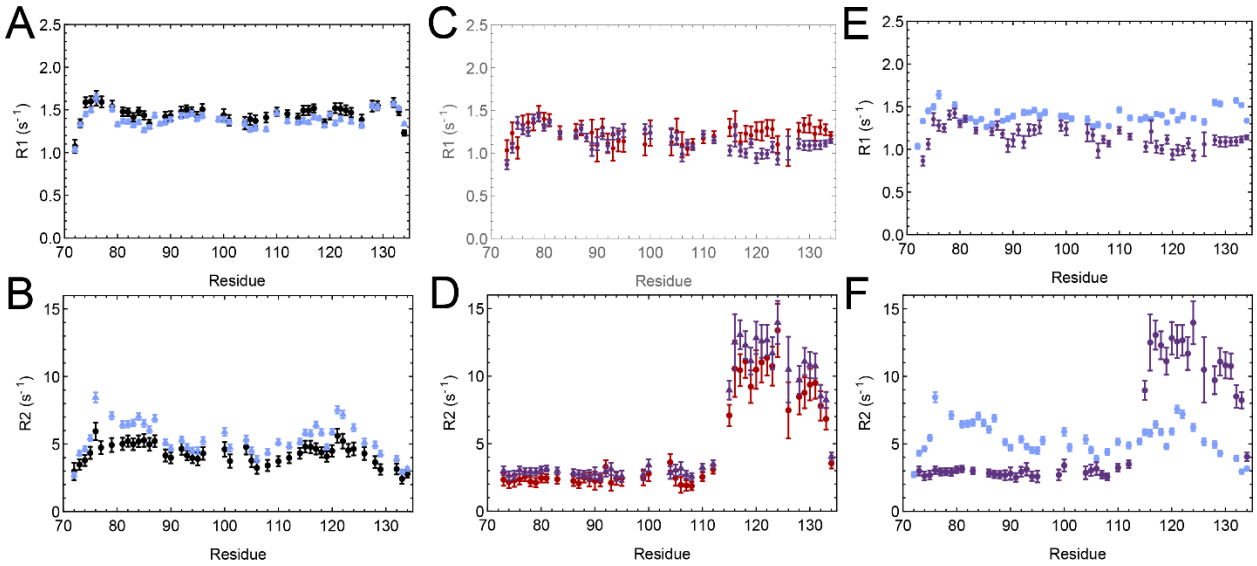

Figure S4 (A) ^{15}N R_1 and (B) R_2 relaxation rates for free mCpx1 CTD were obtained at 10°C at 800 MHz (black) and 900 MHz (blue) field strengths. (C) R_1 and (D) R_2 relaxation rates for DPC micelle-bound mCpx1 CTD were obtained at 40°C at 800 MHz (red) and 900 MHz (purple) field strengths. Comparison of (E) R_1 and (F) R_2 relaxation rates for free (blue) and micelle-bound (purple) mCpx1 CTD at 900 MHz. Similar trends are apparent in the data collected at 800 MHz (Fig. 4).

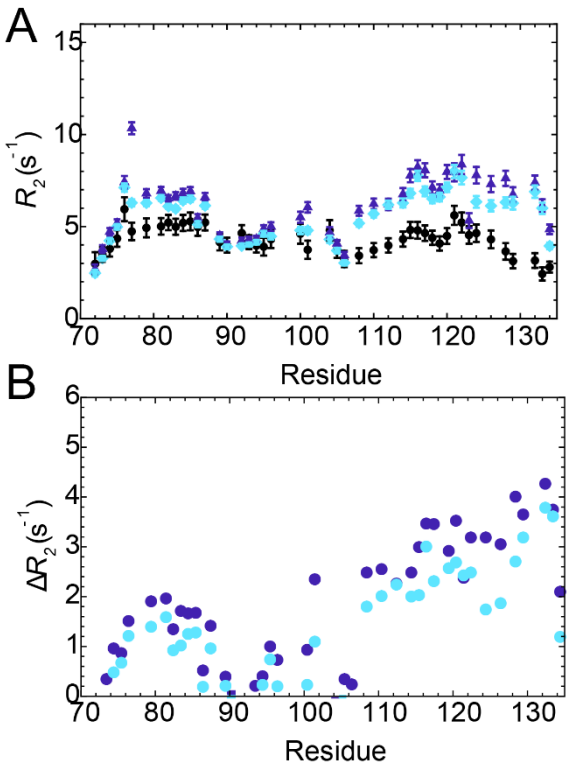

Figure S5 (A) ^{15}N R_2 relaxation rates for mCpx1 CTD in the presence of SUVs composed of 60% DOPC/25% DOPE/15% DOPS (cyan) and 85% POPC/15% POPS (purple) are elevated at the N- and C-termini relative to the free protein (black). All data were collected at 10°C at 800 MHz (^{1}H). (B) ΔR_2 (presence – absence of SUVs) show a significant elevation of relaxation rates in the C-terminus of the mCpx1 CTD in the presence of SUVs and a more modest elevation at the N-terminus of the protein. This effect is observed in both lipid compositions, suggesting that there is no lipid-dependence in the kinetics of the interactions between the mCpx1 CTD and SUVs.

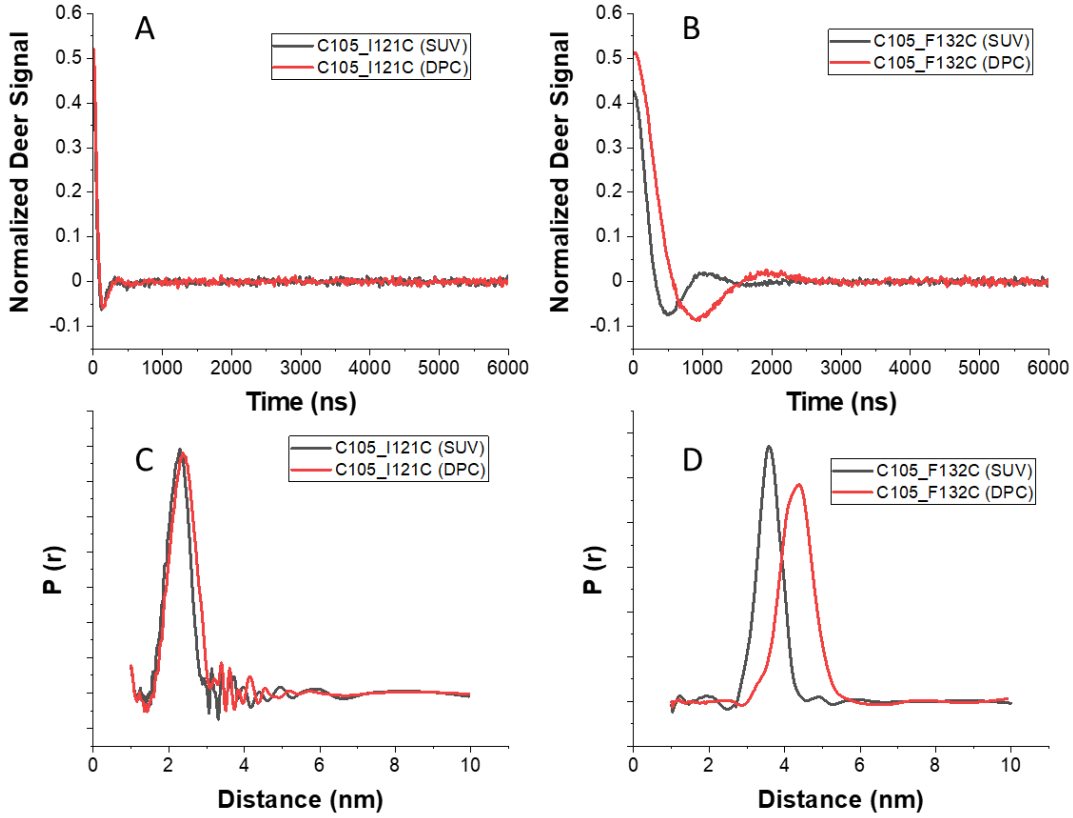

E)

	Peak Position (nm)	Width (nm)
C105_121C in DPC	2.3 ± 0.1	0.8 ± 0.1
C105_121C in SUV	2.3 ± 0.2	0.9 ± 0.2
C105_F132C in DPC	4.3 ± 0.1	0.9 ± 0.1
C105_F132C in SUV	3.5 ± 0.1	0.8 ± 0.1

Figure S6 DEER spectra and the corresponding reconstructed distance profiles. (A and B) Representative normalized experimental DEER spectra for C105-I121C (A) and C105-F132C (B) mCpx1. black: with SUVs (60% DOPC/25% DOPE/15% DOPS) in 1:200 protein/lipid ratio; red, with DPC micelles in 1:200 protein/lipid. (C,D) The corresponding reconstructed distance distribution P(r), of the C105-I121 pair (C, p=0.9462) and the C105-F132C pair (D, p=0.0158). The table E summarizes the distances extracted from the distance profiles. The averages and standard deviations were calculated from three independent experiments. Statistical significance analyses were performed using two-tailed Student's t-tests on the peak positions in the SUV and the DPC micelle distance distributions.

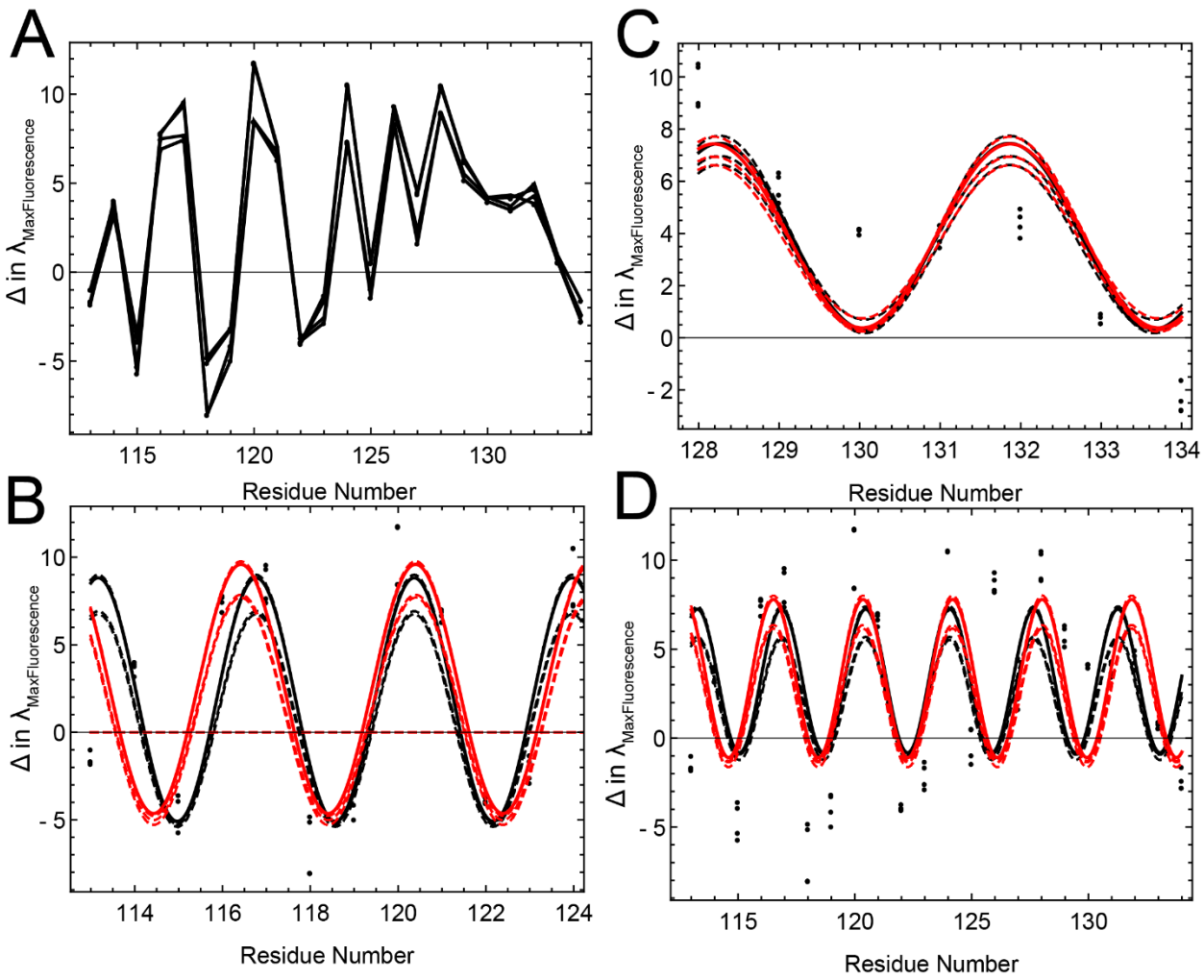

Figure S7 Individual data sets of (A) Shifts in maximum fluorescence wavelength (free - lipid-bound) of Trp-fluorescence wavelength scans for mCpx1 CTD in the absence and presence of SUVs composed of 85% POPC/15%POPS. Four independent data sets are shown. (B) Individual fits to all four datasets for the AH-motif (residues 114-124), (C) for the CT-motif (residues 128-134) and (D) for residues 113-134.

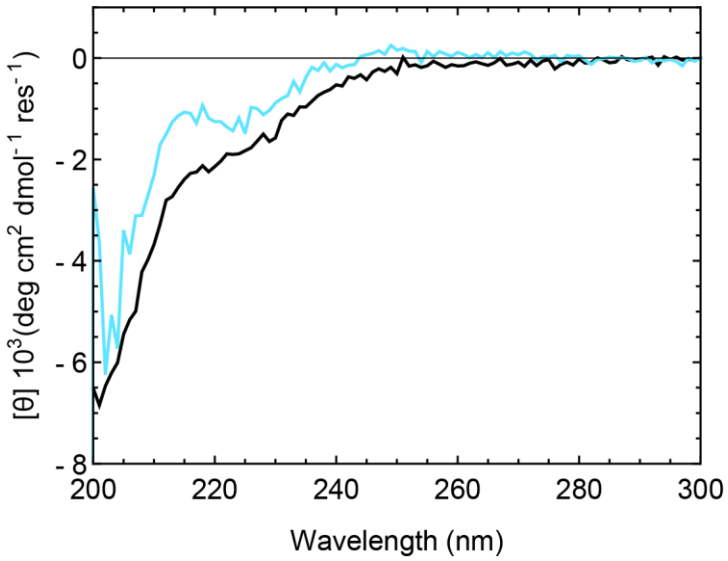

Figure S8 CD spectra for the mCpx1 CTD in the absence (black, 90 μM protein) and presence of LUVs composed of 20 mM 85% POPC/15% POPS (cyan 90 μM protein + 20 mM LUV) are similar to one another and lack the characteristic signals near 208 and 220 nm consistent with the formation of helical structure.

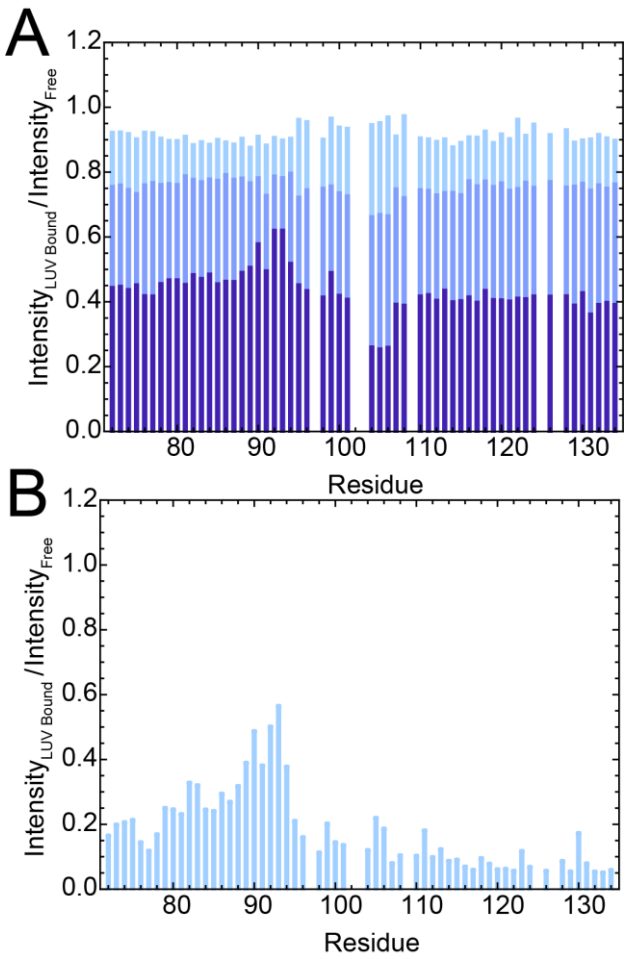

Figure S9 Lipid composition and protein concentrations influence the interaction of mCpx1 CTD with LUVs. (A) Intensity ratios for NMR spectra of mCpx1 CTD (200 μM) in the presence of 0.5 mM (light blue), 1 mM (blue), and 5 mM 60% DOPC/25% DOPE/15% DOPS LUVs (dark blue) show a global decrease in intensity in the lipid-bound state with increasing lipid concentrations, concomitant with the appearance of sample precipitation. 2D {^{15}N-^{1}H} HSQC spectra were collected at 600 MHz (^{1}H) at 10°C with 32 scans and 174 (^{15}N) x 2048 (^{1}H) complex points. (B) At lower protein concentrations (50 μM mCpx1 CTD) and higher lipid concentrations (15 mM LUVs composed of 60% DOPC/25% DOPE/15% DOPS) the ratios of peak heights from NMR spectra show both a global decrease in intensity and localized further decreases at both the N- and C-termini of the CTD. 2D {^{15}N-^{1}H} HSQC spectra were collected at 600 MHz (^{1}H) at 10°C with 256 scans and 174 (^{15}N) x 2048 (^{1}H) complex points in the absence or presence of LUV lipids.